Journal of Engineering Physics and Thermophysics, Vol. 81, No. 5, 2008

CALCULATION OF A TURBULENT MONODISPERSE FLOW IN AN AXISYMMETRIC CHANNEL

B. B. Rokhman

UDC 532.529:532.517.4

A stationary isothermal model of the aerodynamics of a two-phase flow in an axisymmetric channel has been constructed with allowance for the turbulent and pseudoturbulent mechanisms underlying the transfer of the solid phase momentum. The equations of dispersed phase motion are closed at the level of the equations for the second moments of the pulsation velocities of particles, whereas the equation of momentum transfer of the carrier is closed on the basis of a one-parameter model of turbulence extended to the case of two-phase turbulent flows. The results of calculations are compared with experimental data.

Introduction. In view of the complexity of carrying out an experiment aimed at obtaining detailed information on the aerodynamic structure of gas-disperse turbulent flows, of great importance is the construction of mathematical models of such a class of flows and carrying out numerical investigations on their basis. In describing the behavior of particles in rarefied two-phase media (at a low effective concentration of a dispersed phase χ) attention is mainly paid to a turbulent mechanism of solid phase transfer, since the role of the pseudoturbulent component of the energy of random motion of particles owing its origin to interparticle collisions is insignificant. With an increase in the value of χ and in the inertia of particles the contribution of the pseudoturbulent energy to the dispersed phase momentum transfer increases.

In highly concentrated disperse systems, where the kinetic turbulent energy of a gas is small, the determining role in the formation of the statistical properties of the system is played by interparticle interactions. It is assumed that modeling of the interaction of particles is similar to the description of the interaction of the carrier molecules; therefore, the behavior of the solid phase is characterized with the aid of the kinetic theory of dense gases [1]. Here the Enskog equation is used for the velocity distribution function of particles, which is approximated by the Maxwellian distribution function obtained from the Boltzmann equation for a homogeneous stationary state on the condition that the molecular features are additive invariants, even though the system of equations given in [1] is nonstationary and the interparticle collisions are inelastic. Moreover, the Maxwellian distribution function does not account for the coupling between the velocity components, which does not allow one to take into account the redistribution of pulsation energy between them. This property substantially restricts the application of the Maxwellian distribution function. The latter can be used only in the case of an isotropic energy field of the ransom solid phase motion.

Unlike [1], where the approach to the construction of the model was restricted to consideration of the phenomena related only to a pseudoturbulent motion of particles, in [2] an attempt was made to digress outside the scope of the concepts considered by incorporating, into the model of [1], the influence of turbulent effects on the behavior of a two-phase ascending flow in a tube over its stabilized portion using a two-parameter model of turbulence extended to the case of gas-disperse flows. The involvement of particles in the pulsation motion of the carrier medium was taken into account with the aid of a mixed correlation moment $\langle u'_g u'_p \rangle$ appearing in the equations of transfer of k_g, ε_g, and k_p: $\langle u'_g u'_p \rangle = \dfrac{4\delta\xi(u_g - u_p)^2}{\sqrt{\pi}\,\rho_p \beta \sqrt{k_p}}$. From this expression it follows that for $k_p \to 0$ ($\beta \to \beta_{max}$ (the particles are densely packed)) the correlation $\langle u'_g u'_p \rangle \to \infty$. This result is nonphysical, since with $k_p \to 0$ the pulsation velocity of particles tends to zero; consequently, $\langle u'_g u'_p \rangle \to 0$. As to fine particles for which $u_g - u_p \to 0$, this expression suggests

Institute of Coal Power Technologies, National Academy of Sciences and Ministry of Fuel and Power of Ukraine, 19 Andreevskaya Str., Kiev, 04070. Ukraine. Translated from Inzhenerno-Fizicheskii Zhurnal, Vol. 81, No. 5, pp. 844–855, September–October, 2008. Original article submitted May 18, 2007; revision submitted November 18, 2007.

that $\langle u'_g u'_p \rangle \to 0$, although actually $\langle u'_g u'_p \rangle \neq 0$. Thus, the formula considered must have substantial restrictions as to the size of particles and their concentration, although no mention is made of it in [2].

Work [3] presents a kinetic model that simultaneously takes into account turbulent and pseudoturbulent effects. The latter are modeled by the Boltzmann integral operator in Enskog's form. The solution of the kinetic equation for the probability density function was constructed by the perturbation method: the first term of the expansion is the Maxwellian velocity distribution of particles, the second term is expressed as a combination of two particular solutions one of which describes turbulent effect and the other — pseudoturbulent ones.

In the present work, to calculate stationary isothermal motion of a gas-disperse flow in an axisymmetric channel within the framework of so-called two-fluid models, when a gas and a solid phase are considered as interpenetrating interacting solid media, a mathematical model is suggested constructed with the aid of equations for the second moments of the pulsation velocities of particles with allowance for the turbulent and pseudoturbulent mechanisms of solid phase momentum transfer. To calculate the pulsation characteristics of the carrier medium, a modified one-parameter model of turbulence is used which takes into account the influence of particles [4].

Basic Equations. The system of equations that describes the behavior of the ascending gas suspension flow, in the approximation of a two-phase turbulent boundary layer in a circular tube, has the form

$$\frac{\partial (\rho_g u_g)}{\partial z} + \frac{\partial (r \rho_g v_g)}{r \partial r} = 0 , \tag{1}$$

$$\frac{\partial (\beta u_p)}{\partial z} + \frac{\partial [r (\beta v_p + \langle \beta' v'_p \rangle)]}{r \partial r} = 0 , \tag{2}$$

$$\rho_g u_g \frac{\partial u_g}{\partial z} + \rho_g v_g \frac{\partial u_g}{\partial r} = \frac{\partial}{r \partial r} \left[r \rho_g \left(\eta_g \frac{\partial u_g}{\partial r} - \langle u'_g v'_g \rangle \right) \right] - \frac{\partial P}{\partial z} - F_{az} , \tag{3}$$

$$\rho_p \left[\beta u_p \frac{\partial u_p}{\partial z} + \left(\beta v_p + \langle \beta' v'_p \rangle \right) \frac{\partial u_p}{\partial r} \right] = - \frac{\rho_p}{r} \frac{\partial (\beta r \langle u'_p v'_p \rangle)}{\partial r} + F_{az} - \rho_p \beta g, \tag{4}$$

$$\rho_p \left[\beta u_p \frac{\partial v_p}{\partial z} + \left(\beta v_p + \langle \beta' v'_p \rangle \right) \frac{\partial v_p}{\partial r} \right] = - \frac{\rho_p}{r} \frac{\partial [r (v_p \langle \beta' v'_p \rangle + \beta \langle v'^2_p \rangle)]}{\partial r} + F_{ar} + \frac{\rho_p \beta \langle w'^2_p \rangle}{r} , \tag{5}$$

$$\rho_g u_g \frac{\partial k_g}{\partial z} + \rho_g v_g \frac{\partial k_g}{\partial r} = \frac{\partial}{r \partial r} \left[r \rho_g \left(\frac{\eta_{t,g}}{\sigma_k} + \eta_g \right) \frac{\partial k_g}{\partial r} \right] + \rho_g \eta_{t,g} \left(\frac{\partial u_g}{\partial r} \right)^2 - \rho_g (\varepsilon_g + \varepsilon_p) + G_g , \tag{6}$$

$$B_g = 2\pi \int_0^R \rho_g u_g r dr , \tag{7}$$

where

$$\langle \beta' v'_p \rangle = - L_p \frac{\partial \beta}{\partial r} ; \quad \langle u'_p v'_p \rangle = - \eta_{t,p} \frac{\partial u_p}{\partial r} ;$$

$$\langle u'_g v'_g \rangle = - \eta_{t,g} \frac{\partial u_g}{\partial r} ; \quad F_{ar} = \frac{\rho_p \beta}{\tau} (v_g - v_p) ; \quad F_{az} = \frac{\rho_p \beta}{\tau} (u_g - u_p) .$$

In continuity equations (1) and (2) the convective and pulsation transfer of a substance in the axial and radial directions is taken into account. On the right-hand side of the equation of gas motion (3) there are viscous and Reynolds stresses, a pressure gradient, and the inverse effect of particles on the gas. In (4) and (5), the turbulent

stresses, gravity forces and the forces of interphase interaction, as well as the centrifugal force appearing due to the transversal pulsations of the velocity of particles, are taken into account. On the right-hand side of Eq. (6) the first term characterizes the molecular and turbulent transfer of pulsation energy and the second term describes its generation at the expense of the energy of averaged motion, the third term accounts for its dissipation due to the viscosity of the gas phase and of the particles present in it, and the last term characterizes the generation of turbulent energy in the wakes behind the particles.

Equations of Transfer of Second Moments. To close the system of equations (1)–(7), it is necessary to determine the unknown second moments $\langle v_p'^2 \rangle$ and $\langle w_p' w_p' \rangle$ that in turn depend on the Reynolds stresses $\langle w_p' v_p' \rangle$ and $\langle u_p'^2 \rangle$ (see below). To calculate the indicated variables, a specially developed technique of calculation is used based on the construction of the equations of transfer of unknown correlations [5]. According to this technique, the third moments in the equations for double correlations can be found from the truncated equations of transfer of the third moments. Equations for the third-order correlations are closed on the basis of Millionshchikov's hypothesis that presumes the equality to zero of the fourth-order cumulants and represents the fourth moments in these equations as a sum of the products of second moments. This approach allows one to obtain, from the equations for third moments, algebraic relations that express third-order correlations in terms of the second moments and their gradients [5]. Based on this technique, in the approximation of a narrow channel a closed description of momentum transfer in a dispersed phase was obtained at the level of the equations for the second moments of the pulsation velocities of particles:

$$\beta u_p \frac{\partial \langle v_p'^2 \rangle}{\partial z} + \left(\beta v_p + \langle \beta' v_p' \rangle \right) \frac{\partial \langle v_p'^2 \rangle}{\partial r} = \frac{\partial}{r \partial r} \left(r \tau \beta \langle v_p'^2 \rangle \frac{\partial \langle v_p'^2 \rangle}{\partial r} \right)$$

$$- \frac{2\partial \left(\tau \beta \langle w_p' v_p' \rangle^2 \right)}{r \partial r} - 2\beta \langle v_p' v_p' \rangle \frac{\partial v_p}{\partial r} - \frac{2\tau \beta \langle v_p' v_p' \rangle}{3r} \frac{\partial \langle w_p'^2 \rangle}{\partial r}$$

$$- \frac{4\tau \beta \langle w_p' v_p' \rangle}{3r} \frac{\partial \langle w_p' v_p' \rangle}{\partial r} + \frac{4\tau \beta \langle w_p'^2 \rangle^2}{3r^2} - \frac{4\tau \beta \langle v_p'^2 \rangle \langle w_p'^2 \rangle}{3r^2} - \frac{4\tau \beta \langle w_p' v_p' \rangle^2}{3r^2}$$

$$+ \frac{2\beta \left(\langle v_p' v_g' \rangle - \langle v_p'^2 \rangle \right)}{\tau} + 2 \left(G_{pr} - D_r \right), \tag{8}$$

$$\beta u_p \frac{\partial \langle w_p'^2 \rangle}{\partial z} + \left(\beta v_p + \langle \beta' v_p' \rangle \right) \frac{\partial \langle w_p'^2 \rangle}{\partial r} = \frac{\partial}{3r \partial r} \left(r \tau \beta \langle v_p'^2 \rangle \frac{\partial \langle w_p'^2 \rangle}{\partial r} \right)$$

$$+ \frac{2\partial}{3r \partial r} \left(r \tau \beta \langle w_p' v_p' \rangle \frac{\partial \langle w_p' v_p' \rangle}{\partial r} \right) - \frac{2\partial \left(\tau \beta \langle w_p'^2 \rangle^2 \right)}{3r \partial r} + \frac{2\partial \left(\tau \beta \langle v_p'^2 \rangle \langle w_p'^2 \rangle \right)}{3r \partial r}$$

$$+ \frac{2\partial \left(\tau \beta \langle w_p' v_p' \rangle^2 \right)}{3r \partial r} - \frac{2\beta v_p \langle w_p'^2 \rangle}{r} + \frac{2\tau \beta \langle v_p'^2 \rangle \partial \langle w_p'^2 \rangle}{3r \partial r}$$

$$+ \frac{4\tau \beta \langle w_p' v_p' \rangle \partial \langle w_p' v_p' \rangle}{3r \partial r} - \frac{4\tau \beta \langle w_p'^2 \rangle^2}{3r^2} + \frac{4\tau \beta \langle v_p'^2 \rangle \langle w_p'^2 \rangle}{3r^2} + \frac{4\tau \beta \langle w_p' v_p' \rangle^2}{3r^2}$$

$$+ \frac{2\beta}{\tau} \left(\langle w_p' w_g' \rangle - \langle w_p'^2 \rangle \right) + 2 \left(G_{p\varphi} - D_\varphi \right), \tag{9}$$

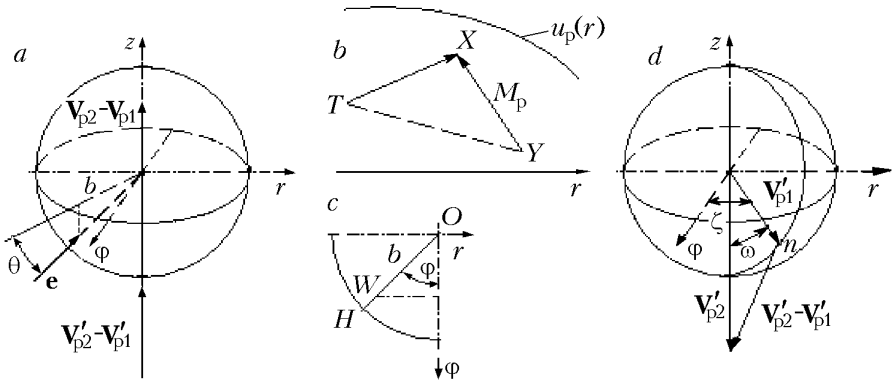

Fig. 1. Toward calculation of the averaged effect of a single impact of monodisperse particles: a) impact geometry; b) scheme of motion of two monodisperse particles before an impact; c) midsection; d) scheme for determining the relative pulsation velocity of particles.

$$\beta u_p \frac{\partial \langle w'_p v'_p \rangle}{\partial z} + \left(\beta v_p + \langle \beta' v'_p \rangle\right) \frac{\partial \langle w'_p v'_p \rangle}{\partial r} = \frac{2\partial}{3r\partial r}\left(r\tau\beta \langle v'^2_p \rangle \frac{\partial \langle w'_p v'_p \rangle}{\partial r}\right)$$

$$- \beta \langle w'_p v'_p \rangle \frac{\partial v_p}{\partial r} + \frac{2\partial (\tau\beta \langle v'^2_p \rangle \langle w'_p v'_p \rangle)}{3r\partial r} + \frac{\partial}{3r\partial r}\left(r\tau\beta \langle w'_p v'_p \rangle \frac{\partial \langle v'^2_p \rangle}{\partial r}\right)$$

$$- \frac{4\partial (\tau\beta \langle w'_p v'_p \rangle \langle w'^2_p \rangle)}{3r\partial r} - \frac{\tau\beta \langle w'_p v'_p \rangle}{r} \frac{\partial \langle w'^2_p \rangle}{\partial r} - \frac{10\tau\beta \langle w'_p v'_p \rangle \langle w'^2_p \rangle}{3r^2}$$

$$- \frac{\beta v_p \langle w'_p v'_p \rangle}{r} + \frac{2\tau\beta \langle v'^2_p \rangle}{3r} \frac{\partial \langle w'_p v'_p \rangle}{\partial r} + \frac{2\tau\beta \langle v'^2_p \rangle \langle w'_p v'_p \rangle}{3r^2}$$

$$+ \frac{\tau\beta \langle w'_p v'_p \rangle}{3r} \frac{\partial \langle v'^2_p \rangle}{\partial r} + \frac{\beta}{\tau}\left(\langle v'_g w'_p \rangle + \langle v'_p w'_g \rangle - 2 \langle w'_p v'_p \rangle\right), \tag{10}$$

$$\beta u_p \frac{\partial \langle u'^2_p \rangle}{\partial z} + \left(\beta v_p + \langle \beta' v'_p \rangle\right) \frac{\partial \langle u'^2_p \rangle}{\partial r} = \frac{\partial}{3r\partial r}\left(r\tau\beta \langle v'^2_p \rangle \frac{\partial \langle u'^2_p \rangle}{\partial r}\right)$$

$$+ 2\tau\beta \langle v'^2_p \rangle \left(\frac{\partial u_p}{\partial r}\right)^2 + \frac{2\beta}{\tau}\left(\langle u'_p u'_g \rangle - \langle u'^2_p \rangle\right) + 2\left(G_{pz} - D_z\right). \tag{11}$$

Mixed correlation moments of the second order (gas–particle) present in Eqs. (8)–(11) are determined in terms of the correlations of the carrier flow in a locally homogeneous approximation according to the recommendations given in [4].

The system of equations (8), (9), and (11) is indeterminate, since it contains additional terms of nonturbulent origin (the last terms of the equations) that describe the generation G_p and dissipation D of the pseudoturbulent energy

of the solid phase caused by interparticle collisions due to the averaged and pulsation movement of particles. These terms cannot be computed by the traditional methods of turbulence theory, since the pulsations related to interparticle collisions depend mainly on the random position of the unit vector **e** (Fig. 1a) directed along the impact line at the given velocity of interacting particles [6].

Generation of Pseudoturbulence. To calculate generation G_p it is first of all necessary to determine the average value of the pseudoturbulent energy acquired by particle 1 as a result of its collision with particle 2. We make the following assumptions: 1) the particles participate in the averaged motion with velocities u_p and v_p (with $v_p << u_p$), therefore we will restrict ourselves to the consideration of only averaged longitudinal velocities of particles, i.e., the vectors $\mathbf{V}_1$ and $\mathbf{V}_2$ are parallel to the z axis; 2) the particles participate in a random motion, the characteristic velocity of which is equal to $\langle \mathbf{V}_p'^2 \rangle^{0.5} = \sqrt{\langle v_p'^2 \rangle + \langle w_p'^2 \rangle + \langle u_p'^2 \rangle}$, with $\langle \mathbf{V}_p'^2 \rangle^{0.5} << u_p$, and the three-dimensional distribution of the vector $\mathbf{V}_p'$ is spherically symmetrical; 3) the main reasons for the collisions are: the difference between the longitudinal averaged velocities of the particles that arrived at the point of interaction X from certain points T and Y (Fig. 1b) and pulsations of $\mathbf{V}_p'$. It is assumed that $|\mathbf{TX}| = |\mathbf{YX}| = M_p = \dfrac{\delta}{6\sqrt{2}\beta}$, and the distribution of the directions of the vectors **TX** and **YX** is equiprobable; 4) we consider the particles to be solid homogeneous spheres; 5) the rotation of the particles is not taken into account, and 6) only binary collisions are considered.

We will analyze the dynamics of a single collision of particles 1 and 2. According to [7], the translational velocity of particle 1 after its collision with particle 2 is equal to

$$\mathbf{V}_{p1}^0 = \mathbf{V}_{p1} + Q\psi_{2,1}(\mathbf{V}_{p2} - \mathbf{V}_{p1}) + A\psi_{2,1}\left[\mathbf{e}(\mathbf{V}_{p2} - \mathbf{V}_{p1})\right]\mathbf{e}, \qquad (12)$$

$$A = 1 - K_n - \frac{2(1 - K_\tau)}{7}, \quad Q = \frac{2(1 - K_\tau)}{7}, \quad K_n < 0.$$

We will project Eq. (12) onto the r axis (see Fig. 1a, c)

$$v_{p1}^0 = A\psi_{2,1}(u_{p2} - u_{p1}) \sin\theta \cos\theta \sin\varphi, \qquad (13)$$

$$\sin\theta = \frac{\sqrt{d^2 - b^2}}{d}, \quad \cos\theta = \frac{b}{d}, \quad b = OW, \quad d = OH = \frac{\delta_1 + \delta_2}{2}, \quad \psi_{2,1} = \frac{m_2}{m_1 + m_2}. \qquad (14)$$

We will integrate the square of expression (13) with allowance for (14) over the south hemisphere, assuming that the probability of intersection of any element of the midsection area of particle 1 by particle 2 is proportional only to the area of this element (i.e., particle 1 is bombarded uniformly). As a result

$$\langle (v_{p1}^0)^2 \rangle = \frac{4}{\pi d^2}\left[A\psi_{2,1}(u_{p2} - u_{p1})\right]^2 \int_0^{\frac{\pi}{2}} \sin^2\varphi d\varphi \int_0^d \left(\frac{b}{d}\right)^2 \left[1 - \left(\frac{b}{d}\right)^2\right] bdb = \frac{[A\psi_{2,1}(u_{p2} - u_{p1})]^2}{12}. \qquad (15)$$

It can be easily seen that $\langle (v_{p1}^0)^2 \rangle = \langle (w_{p1}^0)^2 \rangle$ (by virtue of the symmetry of the problem about the z axis). It should be noted that the average value (rather than the square) of the transverse velocity after an impact is equal to zero. However, the calculation of the average longitudinal velocity of particle 1 yields a result that differs from zero. Let us project Eq. (12) on the z axis:

$$u_{p1}^0 = u_{p1} + (Q + A\sin^2\theta)\psi_{2,1}(u_{p2} - u_{p1}). \qquad (16)$$

Integrating Eq. (16) subject to Eq. (14), we obtain

$$\langle u_{\mathrm{p1}}^{0}\rangle = \frac{1}{\pi d^2}\int_0^{2\pi} d\varphi \int_0^{d}\left\{u_{\mathrm{p1}} + \left[Q + A\left(\frac{d^2 - b^2}{d^2}\right)\right]\psi_{2,1}\,(u_{\mathrm{p2}} - u_{\mathrm{p1}})\right\} bdb = u_{\mathrm{p1}} + \left(Q + \frac{A}{2}\right)\psi_{2,1}\,(u_{\mathrm{p2}} - u_{\mathrm{p1}})\,. \tag{17}$$

The value of the axial component of the pseudoturbulent energy associated with the longitudinal motion and acquired by particle 1 as a result of a single impact is

$$\langle (u_{\mathrm{p1}}^{0} - \langle u_{\mathrm{p1}}^{0}\rangle)^2\rangle = \frac{[A\psi_{2,1}\,(u_{\mathrm{p2}} - u_{\mathrm{p1}})]^2}{\pi d^2}\int_0^{2\pi} d\varphi \int_0^{d}\left(\frac{1}{2} - \frac{b^2}{d^2}\right)^2 bdb = \frac{[A\psi_{2,1}\,(u_{\mathrm{p2}} - u_{\mathrm{p1}})]^2}{12}\,. \tag{18}$$

Thus, from Eqs. (15) and (18) it is seen that generation of pseudoturbulent energy due to the difference of the averaged longitudinal velocities of colliding particles is spherically symmetrical. According to the assumptions made, we should use $M_{\mathrm{p}r}\dfrac{\partial u_{\mathrm{p}}}{\partial r}$ in Eqs. (15) and (18) instead of $u_{\mathrm{p2}} - u_{\mathrm{p1}}$, where $M_{\mathrm{p}r} = M_{\mathrm{p}}/2$ is the average projection of the segment $|\mathbf{TY}|$ on the r axis over all the possible directions of the vectors **TX** and **YX** (Fig. 1b). Then, with allowance for $\psi_{2,1} = 0.5$, Eqs. (15) and (18) will be transformed to give

$$\frac{\langle (u_{\mathrm{p}}^{0} - \langle u_{\mathrm{p}}^{0}\rangle)^2\rangle}{2} = \frac{\langle (v_{\mathrm{p}}^{0})^2\rangle}{2} = \frac{\left(\dfrac{A}{2}\right)^2 \delta^2}{6912\beta^2}\left(\frac{\partial u_{\mathrm{p}}}{\partial r}\right)^2\,. \tag{19}$$

Dissipation of Pseudoturbulence. To calculate the dissipation of pseudoturbulent energy of a solid phase in the direction of the r axis, it is necessary to determine the total energy losses by both colliding particles. We will assume that the vector of the relative pulsation velocity of particles $\mathbf{V}'_{\mathrm{p}2,1} = \mathbf{V}'_{\mathrm{p}2} - \mathbf{V}'_{\mathrm{p}1}$ is parallel to the z axis (this must not change the character of the dependence of the dissipation of the pseudoturbulent energy of particles on K_{n} and K_{τ}). Using Eq. (12), we find the values of $(v'^{0}_{\mathrm{p}1})^2$ for two versions: 1) $K_{\mathrm{n}} = -1$ and $K_{\tau} = 1$ (an absolutely elastic impact of particles with absolutely smooth surfaces (the energy is preserved)):

$$\left(v'^{0}_{\mathrm{p}1}\right)^2_{\mathrm{I}} = 4\psi_{2,1}^2\,\langle\,|\,\mathbf{V}'_{\mathrm{p}2} - \mathbf{V}'_{\mathrm{p}1}\,|\,\rangle^2 \sin^2\theta\cos^2\theta\sin^2\varphi\,; \tag{20}$$

2) $K_{\mathrm{n}} \neq -1$ and $K_{\tau} \neq 1$ (dissipation of turbulent energy takes place):

$$\left(v'^{0}_{\mathrm{p}1}\right)^2_{\mathrm{II}} = A^2\psi_{2,1}^2\,\langle\,|\,\mathbf{V}'_{\mathrm{p}2} - \mathbf{V}'_{\mathrm{p}1}\,|\,\rangle^2 \sin^2\theta\cos^2\theta\sin^2\varphi\,. \tag{21}$$

By averaging the difference between the quantities $(v'^{0}_{\mathrm{p}1})^2_{\mathrm{I}} - (v'^{0}_{\mathrm{p}1})^2_{\mathrm{II}}$ subject to (14), (20), and (21) over the entire range of change of the parameters b and φ, we obtain an expression to determine the total losses of the random energy by both colliding particles:

$$2\,\langle (v'^{0}_{\mathrm{p}1})^2_{\mathrm{I}} - (v'^{0}_{\mathrm{p}1})^2_{\mathrm{II}}\rangle = \frac{2}{\pi d^2}\int_0^{2\pi}\int_0^{d}(4 - A^2)\,\psi_{2,1}^2\,\langle\,|\,\mathbf{V}'_{\mathrm{p}2} - \mathbf{V}'_{\mathrm{p}1}\,|\,\rangle^2\,\frac{b^2(d^2 - b^2)}{d^4}\sin^2\varphi bdb\varphi$$

$$= \frac{(4 - A^2)\,\psi_{2,1}^2\,\langle\,|\,\mathbf{V}'_{\mathrm{p}2} - \mathbf{V}'_{\mathrm{p}1}\,|\,\rangle^2}{6}\,. \tag{22}$$

We note that Eq. (22) can be obtained from (15) if we replace $u_{p2} - u_{p1}$ in it by $\langle |\mathbf{V}'_{p2} - \mathbf{V}'_{p1}| \rangle$ and then, using the expression obtained, we find the difference between the values for two cases: $K_n = -1$, $K_\tau = 1$ and $K_n \neq -1$, $K_\tau \neq 1$.

To find the value of the quantity $\langle |\mathbf{V}'_{p2} - \mathbf{V}'_{p1}| \rangle$ figuring in Eq. (22), we use the known values of $|\mathbf{V}'_{p2}|$ and $|\mathbf{V}'_{p1}|$ and fix the position of the vector $\mathbf{V}'_{p2}$ (Fig. 1d). Here, the point n may occupy any position on the sphere, i.e., the vector of the random velocity $\mathbf{V}'_{p1}$ may have any direction, with these directions being distributed uniformly ($|\mathbf{V}'_{p2}| > |\mathbf{V}'_{p1}|$). Having averaged the expression $|\mathbf{V}'_{p2} - \mathbf{V}'_{p1}| = \sqrt{|\mathbf{V}'_{p2}|^2 + |\mathbf{V}'_{p1}|^2 - 2|\mathbf{V}'_{p2}|\,|\mathbf{V}'_{p1}| \cos\omega}$ over the sphere (see Fig. 1d), we have

$$\langle |\mathbf{V}'_{p2} - \mathbf{V}'_{p1}| \rangle = \frac{1}{4\pi |\mathbf{V}'_{p1}|^2} \int_0^{2\pi} \int_0^{\pi} \sqrt{|\mathbf{V}'_{p2}|^2 + |\mathbf{V}'_{p1}|^2 - 2 |\mathbf{V}'_{p2}|\ |\mathbf{V}'_{p1}| \cos\omega}\ |\mathbf{V}'_{p1}|^2 \sin\omega\, d\omega d\zeta$$

$$= |\mathbf{V}'_{p2}| + \frac{|\mathbf{V}'_{p1}|^2}{3 |\mathbf{V}'_{p2}|}. \tag{23}$$

When $|\mathbf{V}'_{p2}| < |\mathbf{V}'_{p1}|$, $\langle |\mathbf{V}'_{p1} - \mathbf{V}'_{p2}| \rangle = |\mathbf{V}'_{p1}| + \frac{|\mathbf{V}'_{p2}|^2}{3|\mathbf{V}'_{p1}|}$.

Frequency of Collisions. Further we must calculate the sum frequency of N_Σ collisions of monodisperse particles. It includes the frequency N_m originating due to the difference between the averaged axial velocities of particles and the frequency N_h owing its origin to the random motion of particles. Reasoning like in [7], we assume that particle 1 undergoes collisions with particles 2 whose centers at the beginning of the time interval dt are located inside the cylinder with the side $|u_{p2} - u_{p1}|\, dt$ and base $\pi(\delta_1 + \delta_2)^2/4$. Is is assumed that such a cylinder is connected with each particle 1. Then the frequency of the collisions of particles that owe their origin to the difference between their averaged axial velocities, with allowance for the number density of the dispersed phase $\frac{6\beta_2}{\pi\delta_2^3}$, will be equal to

$$N_m = \frac{3(\delta_1 + \delta_2)^2 |u_{p2} - u_{p1}| \beta_2}{2\delta_2^3}. \tag{24}$$

In view of the adopted scheme of motion and interaction of monodisperse particles we transform Eq. (24) using relations $u_{p2} - u_{p1} = M_{pr} \frac{\partial u_p}{\partial r}$, $M_{pr} = \frac{\delta}{12\sqrt{2}\beta}$, and $\delta_1 - \delta_2$. As a result we have

$$N_m = \frac{6\beta M_{pr} \left| \frac{\partial u_p}{\partial r} \right|}{\delta} = \frac{1}{2\sqrt{2}} \left| \frac{\partial u_p}{\partial r} \right|. \tag{25}$$

To calculate the value of N_h the expression $M_{pr} \frac{\partial u_p}{\partial r}$ in Eq. (25) should be replaced by Eq. (23) provided that $|\mathbf{V}'_{p2}| = |\mathbf{V}'_{p1}|$. As a result

$$N_h = \frac{8\beta}{\delta} \sqrt{\langle \mathbf{V}'^2_p \rangle}. \tag{26}$$

To determine the frequency N_Σ, we sum "geometrically" the known values of N_m and N_h with allowance for the fact that the difference between the averaged velocities that leads to collisions N_m is parallel to the z axis, whereas the difference between the random velocities may have any direction, and these directions are distributed equiprobably. Then the value of N_Σ can be found similarly to (23):

$$N_\Sigma = \begin{cases} N_m + \dfrac{N_h^2}{3N_m}, & N_m > N_h; \\ N_h + \dfrac{N_m^2}{3N_h}, & N_h \geq N_m. \end{cases} \tag{27}$$

Using Eqs. (12), (14), (19), (22), (23), and (27) at $\delta_1 = \delta_2$ and $|\mathbf{V}'_{p2}| = |\mathbf{V}'_{p1}|$, we can easily calculate the rates of generation and dissipation of the turbulent energy:

$$G_{pr} = \frac{\left[\dfrac{1-K_n}{2} - \dfrac{1-K_\tau}{7}\right]^2 \delta^2}{6912\beta} \left(\frac{\partial u_p}{\partial r}\right)^2 N_\Sigma, \quad G_{pr} = G_{p\varphi} = G_{pz};$$

$$D_r = C \frac{8\left[1 - \left(\dfrac{1-K_n}{2} - \dfrac{1-K_\tau}{7}\right)^2\right] \langle \mathbf{V}'^2_p \rangle \beta N_\Sigma}{27}, \quad D_r = D_\varphi = D_z. \tag{28}$$

Boundary Conditions and the Algorithm of Calculations. The boundary conditions on the flow axis for Eqs. (1)–(6) and (8)–(11) are prescribed from considerations of symmetry ($r = 0$)

$$\frac{\partial u_g}{\partial r} = \frac{\partial k_g}{\partial r} = \frac{\partial \beta}{\partial r} = v_g = v_p = 0,$$

$$\frac{\partial u_p}{\partial r} = \frac{\partial \langle v'_p v'_p \rangle}{\partial r} = \frac{\partial \langle w'_p w'_p \rangle}{\partial r} = \frac{\partial \langle u'_p u'_p \rangle}{\partial r} = \frac{\partial \langle w'_p v'_p \rangle}{\partial r} = 0, \tag{29}$$

and on the channel wall ($r = R$) by the relations

$$v_p = u_g = k_g = \frac{\partial \beta}{\partial r} = 0, \quad u_p = \frac{\delta}{24\sqrt{2}\,\beta\,(1-K_\tau)} \left(\frac{\partial u_p}{\partial r}\right) (7K_n - 2K_\tau - 5),$$

$$\langle v'_p v'_p \rangle = \frac{K_n \delta}{12\sqrt{2}\,\beta\,(1+K_n)} \left(\frac{\partial \langle v'_p v'_p \rangle}{\partial r}\right), \quad \langle w'_p w'_p \rangle = \frac{\left[K_n - \dfrac{(5+2K_\tau)^2}{49}\right]\delta}{12\sqrt{2}\,\beta\left[1 - \dfrac{(5+2K_\tau)^2}{49}\right]} \left(\frac{\partial \langle w'_p w'_p \rangle}{\partial r}\right), \tag{30}$$

$$\langle w'_p v'_p \rangle = \frac{K_n (6+K_\tau)\,\delta}{6\sqrt{2}\,\beta\,[7 + K_n (5+2K_\tau)]} \left(\frac{\partial \langle w'_p v'_p \rangle}{\partial r}\right), \quad \langle u'_p u'_p \rangle = \frac{\left[\dfrac{(5+2K_\tau)^2}{49} - K_n\right]\delta}{12\sqrt{2}\,\beta\left[\dfrac{(5+2K_\tau)^2}{49} - 1\right]} \left(\frac{\partial \langle u'_p u'_p \rangle}{\partial r}\right).$$

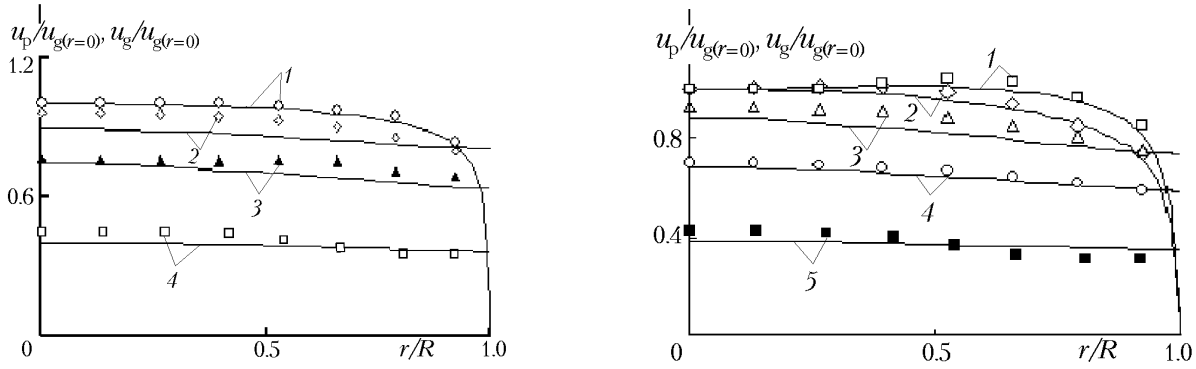

Fig. 2. Profiles of averaged axial velocities of the gas and particles in comparison with the experimental data of [8]: 1) $u_g/u_{g(r=0)}$; 2) $u_p/u_{g(r=0)}$, χ = 4.2, $\delta = 0.2\cdot10^{-3}$ m; 3) $u_p/u_{g(r=0)}$, χ = 3.6, $\delta = 0.5\cdot10^{-3}$ m; 4) $u_p/u_{g(r=0)}$, χ = 3, $\delta = 3\cdot10^{-3}$ m.

Fig. 3. Distribution of averaged longitudinal velocities of the gas and particles over the cross section of an ascending flow in comparison with the experimental data of [8]: 1) $u_g/u_{g(r=0)}$, χ = 3.6, $\delta = 0.5\cdot10^{-3}$ m; 2) $u_g/u_{g(r=0)}$, χ = 2, $\delta = 0.5\cdot10^{-3}$ m; 3) $u_p/u_{g(r=0)}$, χ = 2, $\delta = 0.2\cdot10^{-3}$ m; 4) $u_p/u_{g(r=0)}$, χ = 2, $\delta = 0.5\cdot10^{-3}$ m; 5) $u_p/u_{g(r=0)}$, χ = 2.2, $\delta = 3\cdot10^{-3}$ m.

The complete system of equations (1)–(6) and (8)–(11) with boundary conditions (29) and (30) contains equations of three types. The parabolic equations (2)–(4), (6), and (8)–(11) and hyperbolic equation (5) were integrated by the method of right and left pivots on a nonuniform grid made finer toward the wall. Here, to solve the system (2)–(4), (6), and (8)–(11), the method of iterations was used, whereas for the first-order equation (5) the use of iterations was not needed. The continuity equation of the carrier medium (1) is approximated by an implicit four-point scheme. According to the proposed algorithm a program to calculate two-phase flows has been developed.

Some Results of Calculations. The predicted data as compared to experimental ones [2, 8–10] and models [2, 11] is illustrated by Figs. 2–11, where the profiles of the averaged and pulsation characteristics of an isothermal gas-disperse flow are presented. In Figs. 2–4 the results of calculation of a turbulent gas flow and of monodisperse plastic spherical particles in a vertical tube over a stabilized length are compared with the experimental data of [8] at ρ_p = 1020 kg/m^3, R = 15 mm: $u_{g.m}$ = 14–15.6 m/sec, δ = 0.2 mm; $u_{g.m}$ = 8 m/sec, δ = 0.5 mm; $u_{g.m}$ = 15.3–16 m/sec, δ = 3 mm. It is seen that in the entire range of the effective concentration of particles, their sizes, and of section-averaged velocity of the carrier medium $u_{g.m}$, the model adequately describes the experimental data [8]. Here, the dynamics of the rearrangement of the profile of $u_g(r)$ (the displacement of the maximum of $u_g(r)$ from the axis into the wall region) depending on the value of χ is seen (Fig. 3, curves 1 and 2 are compared). This is associated first of all with the change in the character of the distribution of $\beta(r)$ and $\langle v'_p v'_p\rangle(r)$, $\langle w'_p w'_p\rangle(r)$.

Figure 5 demonstrates the profiles of the dispersed phase concentration and of normal Reynolds stresses $\langle v'_p v'_p\rangle(r)$ and $\langle w'_p w'_p\rangle(r)$ at $u_{g.m}$ = 8 m/sec, δ = 0.5 mm, ρ_p = 1020 kg/m^3, R = 15 mm, χ = 1.1, 3.6 (ascending motion) [8] and $u_{g.m}$ = 20 m/sec, δ = 0.138 mm, ρ_p = 3960 kg/m^3, R = 8 mm, χ = 4.7 (a horizontal flow) [9]. It is seen that at small values of χ, χ = 1.1, the bulk concentration of particles is virtually uniformly distributed over the flow cross section (curve 4), whereas at a maximum flow rate of the solid phase B_p = 97.1 kg/h (χ = 3.6) the behavior of the β(r) curve changes sharply (a maximum on the flow axis and minimum in the peripheral zone (curve 1)). The change in the character of the function β(r) occurs due to the decrease in the pulsation energy of the solid phase (curves 2, 3, and 5, 6 are compared), because of the increase in the rate of dissipation of the pseudoturbulent energy of particles (see Eq. (28)), which in turn leads to a decrease in the intensity of their mixing. Since the maximum of the function β(r) is on the tube axis, the interphase interaction force F_{az} in the axial zone is greater than in the peripheral region, and therefore the carrier medium velocity decreases near the axis and increases in the wall region.

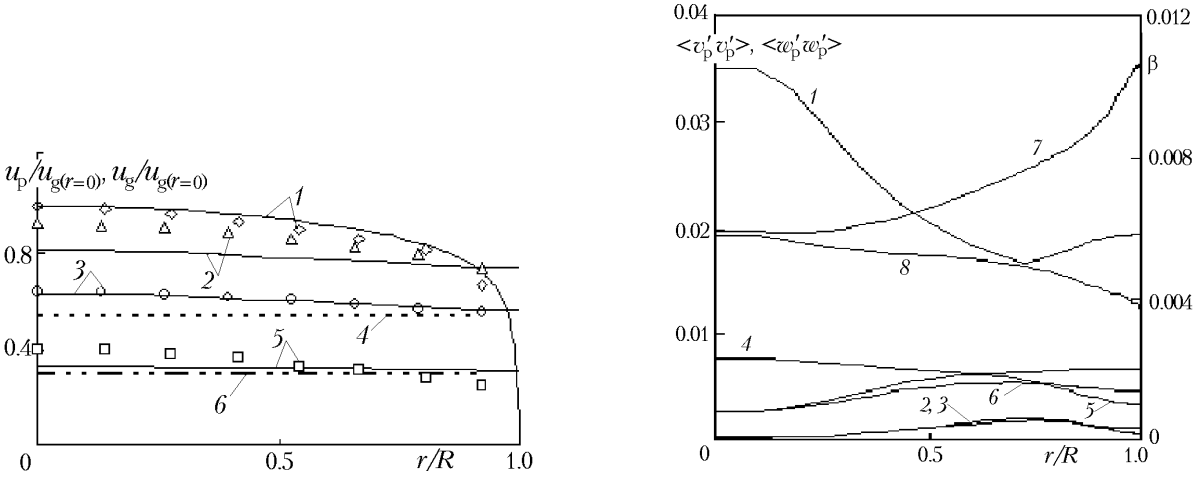

Fig. 4. Distribution of averaged axial velocities of gas and particles over the ascending flow cross section in comparison with the model of [11] and experimental data of [8]: 1) $u_g/u_{g(r=0)}$, $\chi = 1$, $\delta = 3 \cdot 10^{-3}$ m; 2) $u_p/u_{g(r=0)}$, $\chi = 1$, $\delta = 0.2 \cdot 10^{-3}$ m; 3) $u_p/u_{g(r=0)}$, $\chi = 1.1$, $\delta = 0.5 \cdot 10^{-3}$ m; 4) $u_p/u_{g(r=0)}$, $\chi = 1.1$, $\delta = 0.5 \cdot 10^{-3}$ m [11]; 5) $u_p/u_{g(r=0)}$, $\chi = 1$, $\delta = 3 \cdot 10^{-3}$ m; 6) $u_p/u_{g(r=0)}$, $\chi = 1$, $\delta = 3 \cdot 10^{-3}$ m [11].

Fig. 5. Distribution of the bulk concentration of dispersed phase and of second moments of the pulsations of the velocities of particles over the flow cross section: 1) β; 2) $\langle w_p' w_p' \rangle$; 3) $\langle v_p' v_p' \rangle$, $\chi = 3.6$, $\delta = 0.5 \cdot 10^{-3}$ m; 4) β; 5) $\langle w_p' w_p' \rangle$; 6) $\langle v_p' v_p' \rangle$, $\chi = 1.1$, $\delta = 0.5 \cdot 10^{-3}$ m; 7) $\langle w_p' w_p' \rangle$; 8) $\langle v_p' v_p' \rangle$, $\chi = 4.7$, $\delta = 0.138 \cdot 10^{-3}$ m.

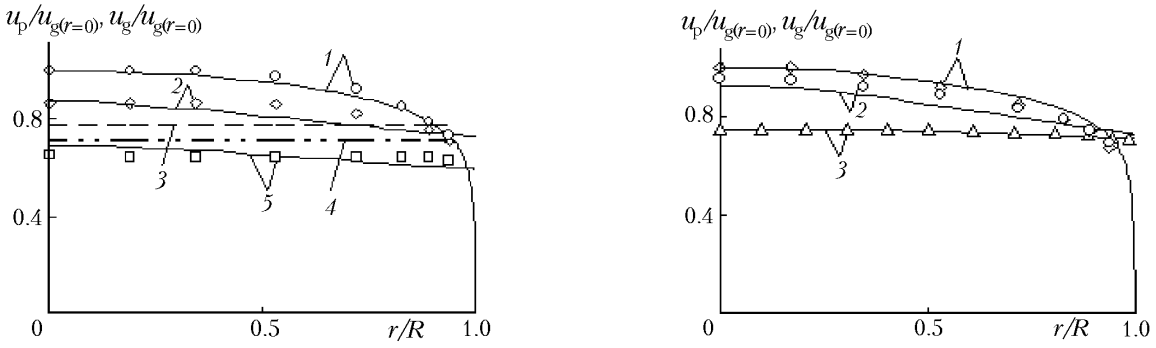

Fig. 6. Profiles of averaged longitudinal velocities of the gas and particles in comparison with the model of [11] and experimental data of [9]: 1) $u_g/u_{g(r=0)}$, $\chi = 0.34$, $\delta = 0.088 \cdot 10^{-3}$ m; 2) $u_p/u_{g(r=0)}$, $\chi = 0.35$, $\delta = 0.044 \cdot 10^{-3}$ m; 3) $u_p/u_{g(r=0)}$, $\chi = 0.35$, $\delta = 0.044 \cdot 10^{-3}$ m [11]; 4) $u_p/u_{g(r=0)}$, $\chi = 0.34$, $\delta = 0.088 \cdot 10^{-3}$ m [11]; 5) $u_p/u_{g(r=0)}$, $\chi = 0.34$, $\delta = 0.088 \cdot 10^{-3}$ m.

Fig. 7. Distribution of the averaged longitudinal velocities of the gas and particles over the horizontal flow cross section in comparison with the experimental data of [9]: 1) $u_g/u_{g(r=0)}$; 2) $u_p/u_{g(r=0)}$, $\chi = 0.34$, $\delta = 0.032 \cdot 10^{-3}$ m; 3) $u_p/u_{g(r=0)}$, $\chi = 4.7$, $\delta = 0.138 \cdot 10^{-3}$ m.

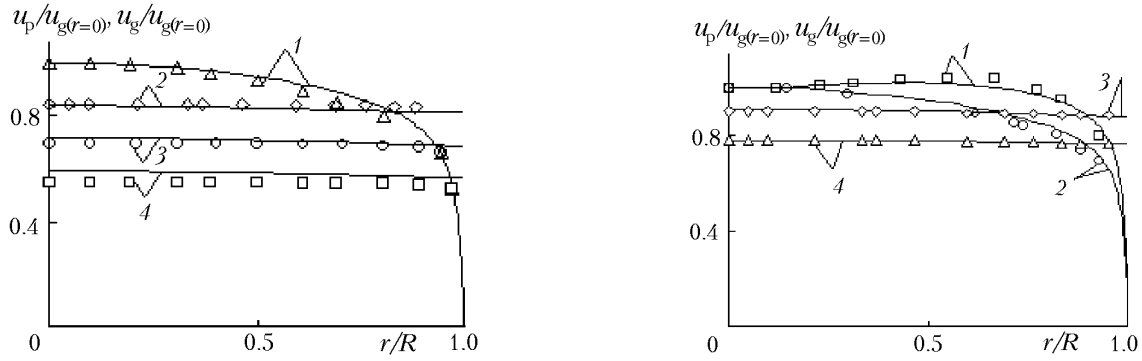

Fig. 8. Profiles of averaged longitudinal velocities of the gas and particles in comparison with the experimental data of [9, 10]: 1) $u_g/u_{g(r=0)}$, χ = 0.65, δ = $0.138\cdot10^{-3}$ m; 2) $u_p/u_{g(r=0)}$, χ = 6, δ = $0.067\cdot10^{-3}$ m; 3) $u_p/u_{g(r=0)}$, χ = 3, δ = $0.138\cdot10^{-3}$ m; 4) $u_p/u_{g(r=0)}$, χ = 0.65, δ = $0.138\cdot10^{-3}$ m.

Fig. 9. Distribution of averaged axial velocities of the gas and particles δ = $0.067\cdot10^{-3}$ m over the horizontal flow cross section in comparison with the experimental data of [10]: 1) $u_g/u_{g(r=0)}$, χ = 14; 2) $u_g/u_{g(r=0)}$, χ = 1.9; 3) $u_p/u_{g(r=0)}$, χ = 14; 4) $u_p/u_{g(r=0)}$, χ = 1.9.

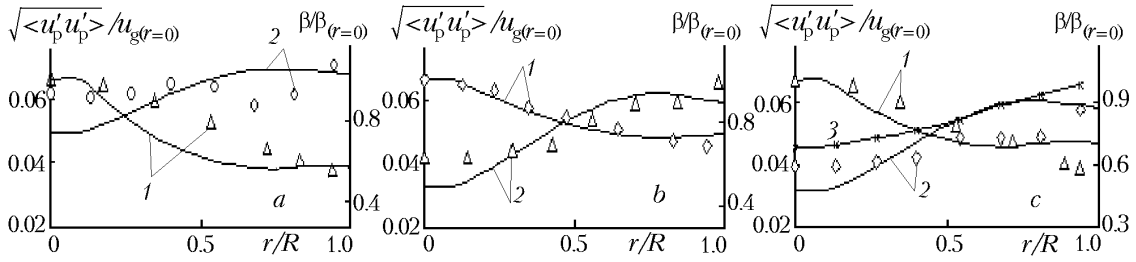

Fig. 10. Distribution of the bulk concentration and axial component of the energy of random motion of particles over the flow cross section in comparison with the experimental data of [2, 9] and model of [2]: a) 1) $\beta/\beta_{(r=0)}$, χ = 0.34, δ = $0.032\cdot10^{-3}$ m; 2) $\sqrt{\langle u'_p u'_p\rangle}/u_{g(r=0)}$, χ = 1, δ = $0.2\cdot10^{-3}$ m; b) 1) $\beta/\beta_{(r=0)}$, χ = 0.34, δ = $0.088\cdot10^{-3}$ m; 2) $\sqrt{\langle u'_p u'_p\rangle}/u_{g(r=0)}$, χ = 3.2, δ = $0.2\cdot10^{-3}$ m; c) 1) $\beta/\beta_{(r=0)}$, χ = 0.35, δ = $0.044\cdot10^{-3}$ m; 2) $\sqrt{\langle u'_p u'_p\rangle}/u_{g(r=0)}$, χ = 4.2, δ = $0.2\cdot10^{-3}$ m; 3) $\sqrt{\langle u'_p u'_p\rangle}/u_{g(r=0)}$, χ = 4.2, δ = $0.2\cdot10^{-3}$ m [2].

Figures 6–8 compare the results of calculation of air flow with corundum particles ρ_p = 3960 kg/m^3 in a horizontal steel tube with experimental data of [9]: δ = 0.032, 0.044, 0.088 mm, χ = 0.34, 0.35, R = 16.8 mm, $u_{g.m}$ = 45 m/sec; δ = 0.138 mm, χ = 0.65, 3, 4.7, R = 8 mm, $u_{g.m}$ = 20 m/sec. It is seen from the figures that the slip velocity of phases $u_g(r) - u_p(r)$ changes substantially over the tube section: it is almost constant in the flow core but decreases closer to the wall and changes sign at a certain distance from it (Fig. 6, curves 1 and 5; Fig. 7, curves 1 and 2; Fig. 8, curves 1 and 4). It should be noted that with increase in the size of particles from 0.032 to 0.088 mm the profile of $u_p(r)$ becomes steeper (Fig. 6, curve 4; Fig. 7, curve 2).

The character of the velocity distribution of particles δ = 0.138 mm is virtually independent of the solid phase flow rate B_p, but with increase in χ, χ = 0.65–4.7, the section-averaged velocity of the dispersed phase increases as a

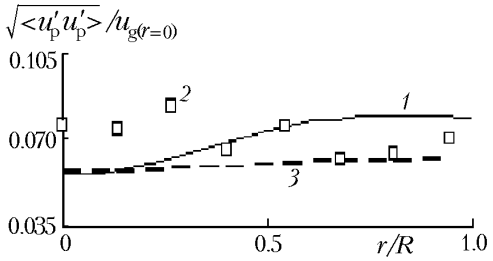

Fig. 11. Distribution of the axial component of the energy of random motion of particles $\sqrt{\langle u'_p u'_p \rangle}/u_{g(r=0)}$ (1) over the ascending flow cross section in comparison with the experimental data of [2] (2) and model of [2] (3) at $\chi = 1.3$, $\delta = 0.2 \cdot 10^{-3}$ m.

result of which the phase slip velocity $u_g(r) - u_p(r)$ decreases (Fig. 7, curve 3; Fig. 8, curves 3 and 4). In contrast to the ascending gas suspension flow ($\delta = 0.5$ mm), where the values of the pulsation energy components of the dispersed phase $\langle w'_p w'_p \rangle$ and $\langle v'_p v'_p \rangle$ are close, in the given case ($\delta = 0.138$ mm) the energy field of the random motion of the solid phase is substantially anisotropic (Fig. 5, curves 2, 3 and 7, 8 are compared).

Figure 6 compares the results of calculation by the proposed technique with the model of [11] (curves 2 and 3, 4 and 5 are compared). It is seen that the present technique describes experimental data more accurately [9].

Figures 8 and 9 compare the results of calculation of air flow with spherical bronze particles in a horizontal axisymmetric stainless steel channel with the experimental data of [10]: $\delta = 0.067$ mm, $\chi = 1.9$, 6, 14, $\rho_p = 8500$ kg/m^3, $R = 8$ mm, $u_{g.m} = 30.5$ m/sec. Just as in the case of the ascending flow of large (but light) plastic particles with $\delta = 0.5$ mm (Fig. 3, curves 1 and 2), here too one sees a clear dependence of the value of u_g on the parameter χ, with increase of which the velocity profile of the carrier medium undergoes similar deformation (Fig. 9, curves 1 and 2 are compared).

Figures 10 and 11 present calculated values of the axial component of the pulsation energy of particles ($\delta = 0.2 \cdot 10^{-3}$ m; $\chi = 1$, 1.3, 3.2, 4.2) and bulk concentration of the dispersed phase ($\delta = 0.032$, 0.044, 0.088 mm, $\chi = 0.34$, 0.35) in comparison with the experimental data of [2, 9] and with the model described in [2]. It is seen that in the entire range of change of the parameters χ, δ, ρ_p, R, and $u_{g.m}$ the model adequately describes the experimental data of [2, 9]. The results of calculations show that the energy of the random motion of particles exceeds the turbulent energy of the gas except for the near-wall zone. With increase in the value of χ the random energy in the axial zone decreases due to the increase in the concentration of particles β in this zone, whereas in the peripheral zone a certain decrease in the pulsation energy of the solid phase is observed (Fig. 10a, c, curves 2 are compared).

Conclusions. Thus, the model proposed in the present work takes into account the turbulent and pseudoturbulent mechanisms of momentum transfer of particles. It allows one to correctly describe the behavior of a two-phase flow in a wide range of change of the parameters χ, δ, ρ_p, R, and $u_{g.m}$. The results of numerical investigations can be of use in calculations of technical facilities intended for pneumatic transportation of loose materials.

NOTATION

A, coefficient; *B*, flow rate, kg/sec; *b*, distance between the vectors of the axial velocities of particles at the moment of impact, m; *C*, empirical constant; *D*, dissipation of the pseudoturbulent energy, m^2/sec^3; *d*, radius of collision cross section, m; **e**, unit vector; *F*, force, kg/(sec^2·m^2); *G*, generation of turbulent (pseudoturbulent) energy, kg/(sec^3·m) for G_g and m^2/sec^3 for G_p; *g*, free fall acceleration, m/sec^2; *K*, coefficient of velocity recovery in impact; *k*, kinetic pulsation energy, m^2/sec^2; *L*, diffusion coefficient, m^2/sec; *M*, mean free path of a particle between successive collisions, m; *m*, mass of a particle, kg; *N*, frequency of impacts, 1/sec; *n*, number density of dispersed phase; *OH* = *d*; *OW*, projection of radius *d* on midsection, m; *P*, gas pressure, N/m^2; *Q*, coefficient; *R*, channel radius, m; *r* and *z*, radial and longitudinal coordinates, m; *t*, time, sec; **TX**, **TY**, **YX**, vectors; *u*, *v*, *w*, averaged components of the velocity vector, m/sec; **V**, vector of particle velocity; β, true bulk concentration of particles; δ, diameter of a particle, m; ε, dissipation of pulsation energy of a gas, m^2/sec^3; η, kinematic viscosity, m^2/sec; θ, φ, ω, ζ, an-

gles; ξ, coefficient of aerodynamic resistance of a particle; ρ, density, kg/m^3; τ, time of dynamic relaxation, sec; ψ, coefficient; χ, B_p/B_g, effective concentration of dispersed phase; σ, empirical constant. Subscripts and superscripts: a, aerodynamic resistance of a particle; g, gas; h, random motion; k, kinetic pulsation energy of a gas; m, mean value; max, limiting value; n, normal; p, particle; t, turbulent pulsations; τ, tangential; φ, transversal coordinate; 1, 2, numbers of particles; I, II, numbers of variants; $'$, pulsation component in time averaging; $\langle\ \rangle$, averaging in time (space).

REFERENCES

1. J. Ding and D. Gidaspow, A bubbling fluidization model using kinetic theory of granular flow, *J. AIChE*, **36**, No. 4, 523–538 (1990).
2. E. J. Bolio, J. A. Yasuna, and J. L. Sinclair, Dilute turbulent gas–solid flow in risers with particle–particle interactions, *J. AIChE*, **41**, No. 6, 1375–1388 (1995).
3. L. I. Zaichik, The kinetic model of particle transfer in turbulent flows with consideration of collisions, *Inzh.-Fiz. Zh.*, **63**, No. 1, 44–50 (1992).
4. A. A. Shraiber, L. B. Gavin, V. A. Naumov, and V. P. Yatsenko, *Turbulent Gas Suspension Flows* [in Russian], Naukova Dumka, Kiev (1987).
5. B. B. Rokhman, Concerning the equations of transfer of the correlation moments of dispersed phase velocity pulsations over a stabilized portion of an axisymmetrical two-phase flow. 1. Equations for second moments. Algebraic relations for third correlations, *Prikl. Fiz.*, No. 2, 11–18 (2006).
6. B. B. Rokhman and A. A. Shraiber, Mathematical modeling of aerodynamics and physicochemical processes in the freeboard region of a circulating fluidized bed furnace. 2. Interaction of particles (Pseudoturbulence), *Inzh.-Fiz. Zh.*, **66**, No. 2, 159–167 (1994).
7. G. L. Babukha and A. A. Shraiber, *Interaction of Polydisperse Material Particles in Two-Phase Flows* [in Russian], Naukova Dumka, Kiev (1972).
8. Y. Tsuji, Y. Morikawa, and H. Shiomi, LDV measurements of an air–solid two-phase flow in a vertical pipe, *Fluid Mech.*, **139**, 417–434 (1984).
9. M. K. Laats and A. S. Mul'gi, Experimental investigations of the kinetic picture of a fine-disperse pipe flow, in: *Turbulent Two-Phase Flows*, Inst. of Thermo- and Electrophysics ESSR, Tallin (1979), pp. 32–46.
10. A. S. Mul'gi, Experimental investigation of a gas flow with homogeneous spherical particles in a tube, in: *Turbulent Two-Phase Flows*, Inst. of Thermo- and Electrophysics ESSR, Tallinn (1979), pp. 47–59.
11. L. I. Zaichik, V. A. Pershukov, M. V. Kozelev, and A. A. Vinberg, Modeling of dynamics, heat transfer, and combustion in two-phase turbulent flows. I. Isothermal flow, *Exp. Thermal Fluid Sci.*, **15**, 291–310 (1997).